Marine Pollution Bulletin 190 (2023) 114842

Contents lists available at ScienceDirect

Marine Pollution Bulletin

journal homepage: www.elsevier.com/locate/marpolbul

Bioaccumulation of selenium in halotolerant microalga *Dunaliella salina* and its impact on photosynthesis, reactive oxygen species, antioxidative enzymes, and neutral lipids

Prabhakar Singh [a], Sakshi Singh [b], Priyanka Maurya [c], Abhishek Mohanta [c], Hardik Dubey [c], Sk. Riyazat Khadim [d], Ankit K. Singh [e], Adarsh K. Pandey [f], Arvind K. Singh [a], Ravi K. Asthana [c,*]

[a] *Biochemistry Department, North Eastern Hill University, Shillong 793022, India*
[b] *Interdisciplinary School of Life Sciences, Institute of Science, Banaras Hindu University, Varanasi 221005, India*
[c] *Centre of Advanced Study in Botany, Banaras Hindu University, Varanasi 221005, India*
[d] *Department of Botany, Model Degree College, Nabarangpur, Odisha 764063, India*
[e] *Department of Botany, Marwari College (a Constituent Unit of Lalit Narayan Mithila University), Darbhanga 846004, India*
[f] *Sophisticated Analytical and Technical Help Institute (SATHI), Banaras Hindu University, Varanasi 221005, India*

ARTICLE INFO

Keywords:
Selenium
Antioxidant
Photosynthesis
Reactive oxygen species
Lipid peroxidation
Proline

ABSTRACT

Selenium (Se) is an essential element for living systems, however, toxic at higher levels. In the present study, *Dunaliella salina* cells were exposed to different Se concentrations for their growth (EC_{50} 195 mg L^{-1}) as well as Se accumulation. The cells exposed to 50 mg L^{-1} Se showed photoautotrophic growth parallel to control and accumulated 65 μg Se g^{-1} DW. A decrease in photosynthetic quantum yield, chlorophyll content, and the increase in intracellular reactive oxygen species, proline content, and lipid peroxidation accompanied by higher neutral lipid accumulation, were recorded at higher Se level. The enzymes superoxide dismutase and catalase played a pivotal role in antioxidative defense. Heterogeneity in accumulated carotenoids at varying concentrations of selenium was prevalent. The cells exposed to 200 mg L^{-1} Se resulted in the disorganization of organelles. Thus, the Se enriched biomass obtained at 50 mg L^{-1} may be explored for bio-fortification of food and feed.

1. Introduction

Selenium (Se) is an essential micronutrient for organisms and showed toxicity at higher doses, through generation of reactive oxygen species (ROS), thus leading even to the oxidation of DNA, its breakage resulting in cell mortality (Letavayová et al., 2006). There is a report of natural water bodies contain 1–10 μg L^{-1} Se (Sohrin and Bruland, 2011), while levels can exceed beyond 50–1000 μg L^{-1} owing to natural and anthropogenic sources such as, agricultural runoffs, industrial waste disposal, atmospheric precipitation, combustion, and mining activities (Pilon-Smits, 2019).

Interestingly, the majority of plants are very sensitive to Se and are non-accumulators, and these can accumulate ≤25 μg Se g^{-1} DW (White et al., 2004). Selenium utilization in microalgae has gained widespread recognition due to their ability to accumulate selenium and transform it into organic forms through sulfur assimilation metabolic pathway

Abbreviations: DW, dry weight; OD, optical density; TEM, transmission electron microscopy; ROS, reactive oxygen species; SeCys, selenocysteine; SeMet, selenomethionine; WHO, World Health Organization; SARS-CoV-2, Severe Acute Respiratory Syndrome Coronavirus 2; GPx, glutathione peroxidases; FDA, Food and Drug Administration; GRAS, generally regarded as safe; MJM, Modified Johnson Medium; PAM-2500, Pulse Amplitude Modulation; NR, Nile Red; DMSO, dimethyl sulfoxide; FCM, flow cytometry; ETRmax, maximum electron transport rate; NPQ, non-photochemical quenching; F0, zero fluorescence; Fm, maximum fluorescence; HR-CRS, High-Resolution Confocal Raman Spectrometer; CCD, charged coupled device; ICP-MS, inductively coupled plasma mass spectroscopy; HPLC, high performance liquid chromatography; EDTA, ethylenediamine tetra acetic acid; PBS, phosphate buffer saline; DCFH-DA, 2,7-dichlorodihydrofluorescien diacetate; DCF, dichlorofluorescein; SOD, superoxide dismutase; CAT, catalase; PMSF, phenylmethylsulfonyl fluoride; PVP, polyvinylpyrrolidone; NBT, nitroblue tetrazolium; TBA, 2-thiobarbituric acid; MDA, malondialdehyde; SPSS, Statistical Package for the Social Sciences; ANOVA, analysis of variance; LPO, lipid peroxidation; ATP, adenosine triphosphate.

* Corresponding author at: Centre of Advanced Study in Botany, Institute of Science, Banaras Hindu University, Varanasi 221005, India.
E-mail address: asthana.ravi@gmail.com (R.K. Asthana).

https://doi.org/10.1016/j.marpolbul.2023.114842
Received 20 December 2022; Received in revised form 10 March 2023; Accepted 14 March 2023

(Gojkovic et al., 2015). Microalgal species such as *Spirulina platensis*, and *Scenedesmus quadricauda* accumulate higher concentrations of Se (Sun et al., 2014). The requirement of Se in algal genera is mainly demonstrated in marine species and is known to protect the cells from oxidative damage (Ekelund and Danilov, 2001).

The Se toxicity in microalgae at higher concentrations may be expressed in changes of reactive oxygen species (ROS), causing lipid peroxidation (LPO) of the cell membranes, oxidation of the proteins and disorganization of cell membranes resulting in cell death (Helliwel and Gutteridge, 1999). The excess dose of Se causes a decline in the growth rate and disruption of the photosynthetic electron transport chain from PSII to PSI in microalgae (Geoffroy et al., 2007). It is well established that the reduction in ROS of the target organisms involved both enzymatic and non-enzymatic components as a strategy of survival.

Se is incorporated as selenoproteins (selenocysteine (SeCys) and selenomethionine (Se-Met)). There are 25 different types of selenoproteins including glutathione peroxidase (GPx) in humans that are known to be involved in oxidoreductions and redox signaling (Saito, 2021). The selenoproteins have implications for human health as low Se status in the diet leads to fatal Keshan (Wang et al., 2021) and Kashin-Beck disease (Loscalzo, 2014), cardiovascular disease (Handy et al., 2021), and Parkinson's disease (Zhang et al., 2019). There is also a report of negative correlation between SARS-CoV-2 replication and the expression of selenoproteins (Zhang et al., 2020). Interestingly, various Asian nations, including India, are reported to be deficient in the Se intake for their adult population (WHO, 2005). However, the daily recommended Se requirement for human adults is nearly 55 μg (Thomson, 2004),

Se bioaccumulation and toxicity in cultures of green microalgal species has been reviewed exhaustively by Gojkovic et al. (2015). The authors concluded that the Se toxicity in terms of EC_{50} values depends on its chemical forms and concentrations showing species specificity. The inorganic water-soluble selenium exists predominantly in natural water bodies as oxyanions-selenate (Se VI, SeO_4^{2-}) and selenite (Se IV, SeO_3^{2-}) (Zhong and Cheng, 2017). Although, selenite and selenate are utilized by microalgal systems differently but, literature indicated that selenate shows a higher toxic effect than selenite. The selenite and selenate upon uptake are reduced to selenide (Se^{-2}) which gets incorporated vis SeCys insertion machinery into proteins and further metabolized to SeMet and SeCyS (Turanov et al., 2011). Se is also the constituent of glutathione peroxidase enzyme (GPx) in microalgae. Selenite is more efficiently utilized as compared to the selenate in the marine microalga *Nannochloropsis oceanica* (Guimarães et al., 2021) selenomethionine (SeMet) is a suitable nutritional supplement due to its higher bioavailability and less toxicity than the inorganic Se (Schrauzer, 2003). The presence of different selenoproteins was also reported by systematic analysis of single-cell eukaryotic selenoproteome of many algal species (Jiang et al., 2020).

The green microalgae *Chlorella* and *Dunaliella* species account for approximately 50 % of global microalgal biomass production (Becker, 2007). A study with *Chlorella* sp. indicated that it is a potential alternative source of organically bound Se for food supplementation (Gojkovic et al., 2014). A study on *Chlorella vulgaris* estimated the effective concentration of Se to be ≥75 mg L^{-1}, whereas a reduced level accelerated its antioxidative potential by positively promoting the growth of *C. vulgaris* (Sun et al., 2014). Se-enriched microalga *C. pyrenoidosa* positively promoted algal growth at lower concentrations (≤40 mg L^{-1}) of Se (Zhong and Cheng, 2017). In mice fed with Se-enriched *C. sorokiniana*, the selenium bioavailability was 1.13 fold higher compared to the basal diet suggesting it to be used as a functional food (Gómez-Jacinto et al., 2020). Se (IV) is also reported to alleviate Cr (VI) toxicity in another microalga *Chlamydomonas reinhardtii* through its scavenging effect on ROS production (Zhang et al., 2021). Thus, Se is not only getting transformed into useful selenoproteins but also takes part in the removal of ROS up to the critical threshold limit of Se concentration.

D. salina, a halotolerant chlorophyte, accumulates a high carotenoid, lipid, and protein content under conditions that are sub-optimal for growth, such as high light intensity, sub-optimal temperatures, nutrient limitation, and high salt concentrations. It is one of the richest source of natural carotenoids (up to 10 % of dry biomass), and has been classified by the US Food and Drug Administration (FDA) as a food source, generally regarded as safe (GRAS) status (Sui and Vlaeminck, 2020). The dry biomass of *D. salina* in bread and pasta has enhanced nutritional properties such as high protein and mineral contents. *D. salina* biomass itself has not been reported to be toxic till to date as the *D. salina* powder reversed the hepatic fibrosis in rats because of the hepatoprotective and antioxidative activity (El-Baz et al., 2020). In spite of nontoxic nature of *D. salina* biomass, Se-enriched *Dunaliella* harvested at particular Se concentration must be subjected to toxicity tests before recommending the use in general. This is because Se at higher levels may cause toxicity as demonstrated in a tilapia fish (*Oreochromis mossambicus*) (Gobi et al., 2018; Gopi et al., 2021). These workers assessed the impact of environmentally relevant concentrations of Se toxicity, 5, 10, 25, 50, and 100 mg L^{-1} or water only (control) for period of 4 d. Higher Se concentrations inhibited the acetyl choline esterase activity in brain tissues. Thus, there is a little exploration of the optimum Se level to produce a Se-enriched *D. salina* biomass to be used for biotechnological purposes and the same is not inhibitory to *D. salina* itself. Therefore, the objective of the present study was to examine the halotolerant *D. salina* for its tolerance towards the graded concentration of Se *vis a vis* its accumulation in Se exposed cells. The physiological status of such cells with special reference to photosynthetic parameters, organization of thylakoids and photopigments, lipid peroxidation, proline, neutral lipid content along with antioxidative enzymes (SODs and CATs).

2. Materials and methods

2.1. Culture conditions and Se treatment

The strain *D. salina* was isolated from Sambhar Lake, Rajasthan, India (26°58′ N, 75°05′ E) and cultivated in Modified Johnson Medium (MJM) amended with 2 M NaCl. The isolated strain was identified as *D. salina* morphologically and the molecular identification was based on 18 s rDNA amplification and sequencing as described by Singh et al. (Singh et al., 2019). The exponentially growing *D. salina* cells (100 mL) were poured into 250 mL flasks, followed by addition of 25, 50, 100, 200, and 500 mg L^{-1} sodium selenite (Na_2SeO_3) (Himedia, Nasik, India) as a source of Se. The culture without Se acted as a control. The cultures were maintained at 100 μmol m^{-2} s^{-1} illumination, 16/8 h light-dark cycle, and at a temperature of 25 ± 2 °C. The cultures with three replicates were shaken periodically.

2.2. Growth measurement and toxicity test

The growth of *D. salina* cells exposed to varying Se concentrations (0, 25, 50, 100, 200, 500 mg L^{-1} Se), as described in Section 2.1, was measured in terms of absorbance at 750 nm (OD) and Chl *a* content. These measurements, including carotenoid content, were performed as described by Myers and Kratz (Myers and Kratz, 1955). *D. salina* cells exposed to varying Se concentrations were also monitored for EC_{50} calculation on the basis of percent survival. The culture OD and cell number were monitored at every alternate day up to 6 d.

2.3. Measurement of chlorophyll fluorescence parameters

Chlorophyll fluorescence parameters like *Fv/Fm*, *ETRmax*, NPQ, Y (II), Y(NPQ), Y(NO), qP, qN, and qL were measured by using pulse amplitude modulated fluorometer PAM-2500 (Walz, Effeltrich, Germany). The selenium-treated exponentially grown algal samples were dark-adapted for 20 min. The zero-fluorescence level (Fo) was measured at 0.001 μmol m^{-2} s^{-1} after turning off the actinic light. Maximum fluorescence level (Fm) was measured using a saturating pulse of 3000 μmol m^{-2} s^{-1}.

2.4. Chlorophyll quantification using flow cytometry (FCM) analysis

The Nile red (9-diethyl amino 5-hexabenzo α-phenoxazine-5-one (NR)) was procured from Sigma, USA. The stock solution of NR stain (0.5 mg mL^{-1} was prepared in dimethyl sulfoxide (DMSO). A 5 μL of this solution was added to 1.0 mL selenium treated *D. salina* cells (0.6 OD at 750 nm) and incubated under darkness for chlorophyll staining. Flow cytometry analysis (FCM) was carried out using Beckman Coulter (CytoFlex LX) equipped with 488 and 633 nm lasers. Low-fluorescence cell events (APC 200 AU) were considered debris. The chlorophyll fluorescence measurements were performed using the fluorescence filter known as APC (670/30 nm excited at 633 nm). The obtained data were analyzed online using the software (https://www.flowjo.com/).

2.5. Raman spectroscopy

A High-Resolution Confocal Raman Spectrometer (HR-CRS) (Witec alpha 300 RAS, Ulm, Germany) with a confocal microscope (Witec) and a Zeiss Epiplan 50×/0.65 objective was used to acquire the spectra. It was done using a charged coupled device (CCD) detector with an excitation wavelength of 532 nm. Each spectrum was tested 10 times, and the capture time was 1 s. The spectral range for the chosen microalga was 400 to 1800 cm^{-1}. The *Dunaliella* cells were chosen under the microscope based on their physical state. There were variations in total spectra with changes in the size of microalga.

2.6. Transmission electron microscopy

The control and treated microalgal cells were washed with phosphate buffer saline (1× PBS; pH 7.2) and fixed in 2.5 % glutaraldehyde prepared in sodium cacodylate (Ladd Research Industries, USA, Burlington) buffer (pH 7.2) for 2 h at 4 °C. The cells were washed three times in 0.1 M sodium cacodylate buffer and post fixed in 1 % osmium tetroxide for 4 h. Fixed cells were washed with sodium cacodylate, dehydrated in acetone series (15–100 %), and embedded in araldite-DDSA mixture (Ladd Research Industries, USA, Burlington). After baking at 60 °C, blocks were cut (60–80 nm thick) by an ultramicrotome (Leica EM UC7) and sections were stained by uranyl acetate and lead citrate. Analysis of sections was done under FEI Tecnai G2 spirit twin. The transmission electron microscope was equipped with Gatan digital CCD camera (Netherland) at 80KV.

2.7. Intracellular Se content

The total Se was determined using inductively coupled plasma mass spectrometry (ICP MS) (PerkinElmer® Optima™ 7000 DV, Waltham, USA) (Zheng et al., 2017). The treated *D. salina* cells were centrifuged at 8000 rpm (1 min) at room temperature. The cell pellets were washed using EDTA and then lyophilized. The lyophilized biomass (5 mg) of each sample was digested with concentrated nitric acid (6 mL) and hydrogen peroxide (2 mL) in a digestion unit at 180 °C for 3 h. After digestion, the solution was diluted with ultra-pure water (HPLC grade) to a final volume of 10 mL and analyzed directly for total Se content by ICP MS.

2.8. Reactive oxygen species (ROS) assay

Cell permeable non-fluorescent probe 2,7-dichlorodihydrofluorescein diacetate (DCFH-DA; Sigma-Aldrich, USA) was used for in vivo detection and quantification of ROS (He and Häder, 2002). *D. salina* cells (0.6 OD) exposed to different selenium concentrations were subjected to DCFH-DA (5 μM) followed by 30 min incubation in a dark room at room temperature. These samples were washed thoroughly in PBS (50 mM, pH 7.0), and stained cells were analyzed using a fluorescence microscope (Nikon ECLIPSE 90 i, Melville, NY, USA) having NIS-Elements 4.0 software. Imaging in the epifluorescence mode with a 20× objective lens was used with similar exposure times for all samples. Green (G) and red (R) fluorescence intensities were obtained for randomly selected cells.

2.9. Antioxidant enzymes assay

In-gel assay of superoxide dismutase (SOD) and catalase (CAT) was performed as described by Weydert and Cullen (Weydert and Cullen, 2010).

2.9.1. Preparation of enzyme extract

Dunaliella cells (40 mL) were centrifuged (5000 rpm, 5 min, 4 °C). The pellet was washed thoroughly in extraction buffer (potassium phosphate buffer (100 mM), EDTA (1 mM), PMSF (1 mM), and PVP (1 %)). The sample was homogenized in extraction buffer (1 mL) at low temperature by sonication (20 % amplitude, 10 s pulse for 5 min). The supernatant obtained was used for in-gel antioxidative enzyme (SOD and CAT) assay. Total soluble protein content was determined by Bradford assay (Bradford, 1976) using bovine serum albumin (BSA) as standard. The extracted proteins were electrophoretically separated on native polyacrylamide gels (10 %) and analyzed for in-gel SOD activity. The gel was soaked in riboflavin-NBT solution (riboflavin 0.1 mg mL^{-1}, nitro blue tetrazolium (NBT 0.25 mg mL^{-1}) and kept in the dark at RT for 10–15 min. After draining riboflavin-NBT solution from the gel, TEMED (0.1 %) was added and incubated further at RT for 15 min in the dark and placed under light till distinct bands of SOD appeared (within 15–20 min). For the catalase assay, the gel was treated with H_2O_2 (0.003 %) for 10 min, washed with distilled water, followed by staining with ferric chloride (1 %) and potassium ferricyanide (1 %). The catalase activity was observed as a zone of clearance on a greenish-yellow background of the gel. The achromatic bands appeared within 10–15 min.

2.10. Neutral lipid analysis

The NR stain was used to detect neutral lipids in *D. salina* cells (Yilancioglu et al., 2014). A fluorescence spectrophotometer (Cary Eclipse, Agilent, USA) was used to quantitatively determine neutral lipids, with the excitation and emission wavelengths being 485 nm and 612 nm, respectively. NR-stained *D. salina* micrographs with significant golden yellow emissions (lipid bodies) were captured using Zen 2010 imaging software and a Zeiss LSM 780 laser-scanning confocal microscope (Carl Zeiss, GmbH, Germany), with a common exposure time and excitation and emission wavelength were at 525 and 595 nm, respectively (Singh et al., 2019).

2.11. Lipid peroxidation assay

The total 2-thiobarbituric acid-reactive substances (TBA) as a marker of lipid peroxidation were represented as malondialdehyde (MDA) equivalents (Dhindsa and Matowe, 1981). *D. salina* cells were harvested and homogenized in 3 mL solution containing 20 % TCA and 0.5 % TBA. The homogenate was then incubated for 30 min at 100 °C. The reaction mixture was rapidly cooled, and centrifuged (9300*g*, 10 min), followed by absorbance measurement at 532 nm. The nonspecific turbidity was corrected by subtracting the absorbance at 532 nm from the absorbance at 600 nm. The extinction coefficient (155 mM^{-1} cm^{-1}) was used to determine the MDA content.

2.12. Proline estimation

Intercellular free proline was measured as per Bates et al. (Bates et al., 1973). The *D. salina* cells were centrifuged and re-suspended in 10 mL of sulfosalicylic acid (SRL, Mumbai, India), followed by sonication for 5 min using ultrasonicator (Sonics, USA). The broken cell suspension was centrifuged to remove cell debris. The proline in the resulting supernatant was determined by the acid ninhydrin method. Proline

concentration was determined from the standard curve prepared by dissolving proline in 3 % (v/v) sulfosalicylic acid.

2.13. Statistical analysis

Each experiment was performed in triplicates, and the data were presented as the mean ± SD. One-way ANOVA with Duncan's multiple range test ($P \leq 0.05$) was used in the SPSS statistical software (Version 20.0; SPSS Inc. Armonk, NY, USA) to determine the statistical significance of the treatments.

3. Results and discussion

3.1. Photoautotrophic growth, evaluation of 50 % growth inhibition and bioaccumulation of Se in D. salina

The exponentially growing *D. salina* cells were treated with varying Se concentrations followed by photoautotrophic growth measurement, by recording absorbance daily at 750 nm for 6 d (Fig. 1A). The *D. salina* cells growing at 100, 200, and 500 mg L^{-1} Se turned reddish on 4th d after exposure (Fig. S1). Microscopic examination of the cells derived from such cultures showed a change in their shape through incremental progression to sub-spherical (Fig. S1). The toxicological effects of Se in *D. salina* were assessed by analyzing 50 % growth inhibitory concentration (EC_{50}) from the dose response curve (Fig. S2). It was calculated as 195 mg L^{-1} after 6 d. Another strain of *D. salina* originating from China also showed 50 % growth inhibition of the strain at 192.7 mg L^{-1} after 11th d (Jiang et al., 2023 Feb 13). EC_{50} values for Se (as selenite) against microalgal systems varied from 4 mg L^{-1} to 302 mg L^{-1} even varying in different species of same genera as enlisted by Guimarães et al. (Guimarães et al., 2021). These algal genera belong to various *Chlorella*, *Desmodesmus*, *Nannochloropsis*, *Selenastrum*, *Scenadesmus*, and *Pseudokirchneriella*. Therefore, overall toxicological differences in microalgae towards Se depends on the type of species involved in the study. However, higher EC_{50} level in the present study indicated the inherent characteristic feature of *D. salina* to withstand Se stress. The Chl *a* and carotenoid pigments reached their maxima in control and cultures treated with 25 and 50 mg L^{-1} Se 6th d after inoculation. This result shows 50 mg L^{-1} Se as a nontoxic concentration. However, Se at 100, 200, and 500 mg L^{-1} concentrations, led to a decline in absorbance, and Chl *a* with increase in carotenoid levels. These results are in agreement with previous reports on microalga, showing Se toxicity at higher concentrations i.e., >100 mg L^{-1} in *C. vulgaris* (Sun et al., *2014)* and >60 mg L^{-1} in *C. pyrenoidosa* (Zhong and Cheng, 2017) indicating species specificity. Some microalgae such as *Emiliania huxleyi* (173 μg L^{-1}) (Gojkovic et al., 2015), *C. vulgaris* (≥75 mg L^{-1}) (Sun et al., 2014), *C. pyrenoidosa* (≥40 mg L^{-1}) (Zhong and Cheng, 2017) require Se for better growth. These microalgae grew better at reduced Se concentrations, whereas *D. salina* cells grown in 2 M NaCl (control) containing media tolerated Se up to 100 mg L^{-1}. Recently, other microalgal strains *Scenedesmus* and *Chlorella* were used directly to sequester Se from the wastewater and tolerated up to 1 mg L^{-1} Se only from the contaminated environment (De Morais et al., 2022). In comparison, the *D. salina* strain in the present study showed higher tolerance as it was healthy up to 50 mg L^{-1} Se exposure. These workers also reported that *Chlorella* accumulated 323 μg Se g^{-1} DW while *D. salina* grown at 200 mg L^{-1} Se containing culture media accumulated 2262 μg Se g^{-1} DW, indicating *D. salina* as a hyper-accumulator of Se. This finding emphasized the significance of *D. salina* in the bioremediation of Se contaminated environment.

3.2. Effect of Se on photosynthetic parameters

The photosynthetic status of *D. salina* exposed to Se from 0 to 500 mg L^{-1} concentrations were evaluated for 6 d. The maximum photochemical quantum yield (*Fv/Fm*) above 0.6 is suggestive of photosynthetically active and viable microalgal cells, indicating maximum efficiency of reducing QA photosystem II as described by Butler (Butler, 1978). A decline in *Fv/Fm* value was observed at higher Se levels (100, 200, and 500 mg L^{-1}), 4 d after treatment (Fig. 2A). Similar result was reported for the microalga *Haematococcus pluvialis* (Zheng et al., 2017). The *Fv/Fm* values were maintained near (~0.6) till 50 mg L^{-1} selenite for 6 d. In contrast, a significant decline in *Fv/Fm* values occurred with an average 2.2 fold in 100 (1.78 fold), 200 (2.64 fold) and 500 mg L^{-1} (2.23 fold) Se treated cells compared to control (Fig. 2A). Se being sulfur analog probably inhibits electron transport from PS II to PS I by competing with sulfur in Fe−S complex of the Cyt b6f complex (Geoffroy et al., 2007)). As the water splitting complex is linked to PS II, the Se interference with the photosynthetic electron transfer chain indirectly impacts the rate of O_2 evolution. Exposure of *C. reinhardtii* to 10 μM selenate concentration caused a decline in maximal quantum yield at 66 % and effective photochemical productivity of PS II at 83 % after 96 h (Geoffroy et al., 2007). The overall response of *D. salina* suggests 50 mg L^{-1} selenite as the optimum concentration for biomass production.

The maximum electron transport rate (ETRmax) represents effective photochemistry and is expressed as μmol electrons m^{-2} s^{-1}. The electron transport rate of *D. salina* cells at different Se concentrations is presented in Fig. 2B. The increase in ETRmax till 3rd d and decline thereafter in cells exposed to 100, 200, and 500 mg L^{-1} Se in comparison to control may be attributed to the stress caused by Se at higher doses.

The non-photochemical quenching (NPQ) value is indicative of the

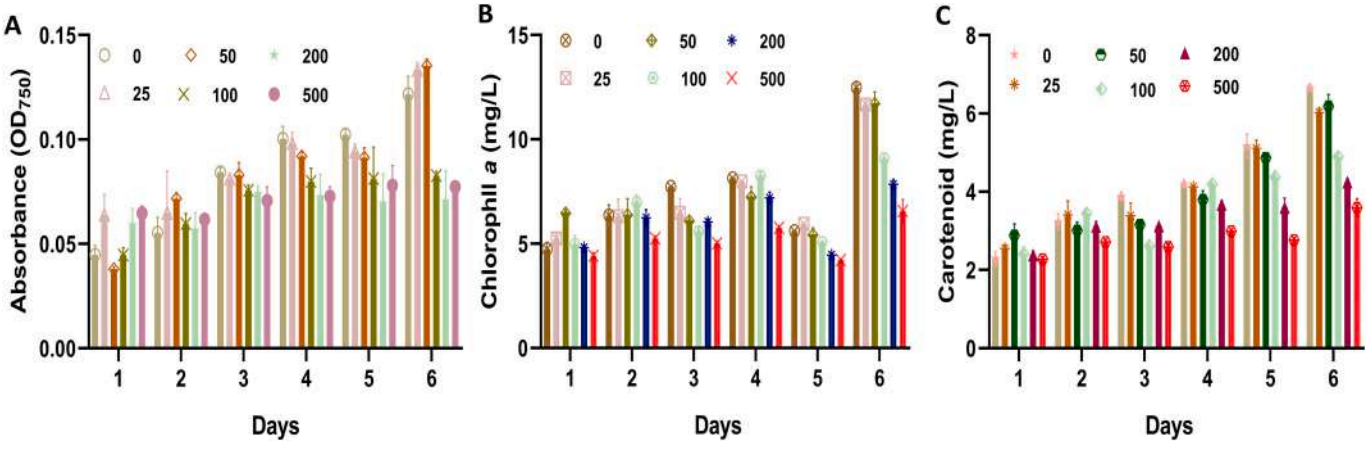

Fig. 1. Photoautotrophic growth of *D. salina* under varying levels of Se (0, 25, 50, 100, 200 and 500 mg L^{-1}): (A) Culture density, (B) Chl *a*, and (C) carotenoid content.

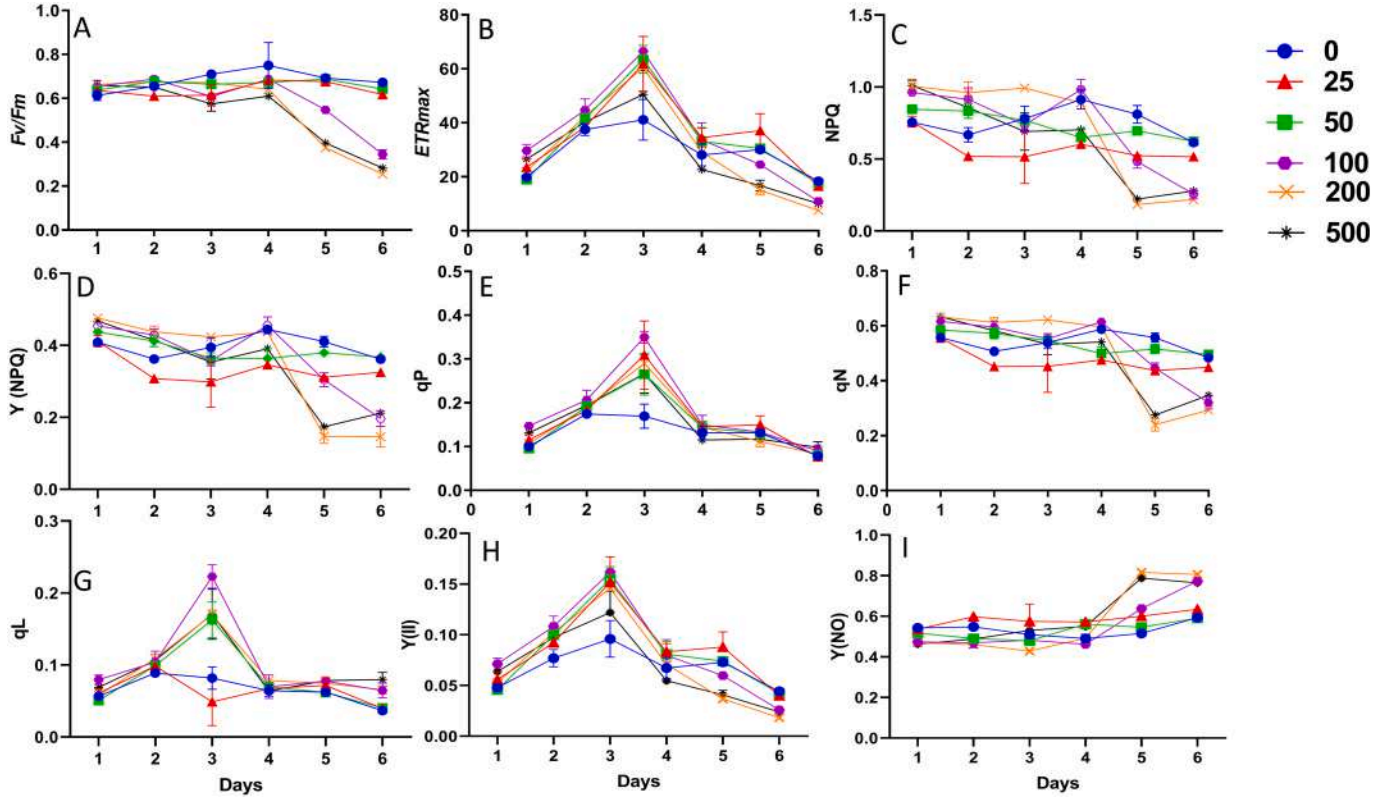

Fig. 2. Effect of varying level of Se (0–500 mg L^{-1}) on photosynthetic parameters of *D. salina*: (A) *Fv/Fm*, (B) *ETRmax*, (C) NPQ, (D) Y(NPQ), (E) qP, (F) qN, (G) qL, (H) Y(II) and (I) Y(NO).

quenching process in the form of maximum heat dissipation highlighting, the photoprotective mechanisms of PS II other than photochemistry. It is associated with the number of quenching centres in the light-harvesting antenna and monitors the apparent rate constant for heat loss. It was evident that the NPQ values declined in 100, 200, and 500 mg L^{-1} Se treated cells (Fig. 2C) compared to control on 6th d after incubation. It was observed that with the increase in Se concentration, the Y(NPQ) value increased initially, followed by a gradual decline compared to control on 6th d (Fig. 2D). Thus, the energy dissipation pattern causing yield loss at higher Se concentrations is evident from the increase in Y(NO) accompanied by a reduction in Y(NPQ) levels, indicating the photo-protective damage (Schreiber and Klughammer, 2008). The Y(II) is effective photochemical quantum yield of PS II mainly due to closed reaction centres (Klughammer and Schreiber, 2008). This explained the decline in Y(II) at the higher Se concentration compared to control on 6th d (Fig. 2F). The Y(NO) determines the quantum yield of non-regulated energy dissipation of PS II. Y(NO) values continued to increase all through the 6th d when cells were exposed to higher Se concentration (Fig. 2I), indicating thereby the decline in photosynthetic activity. The quantum yield, Y(NO), and Y(NPQ) values under Se exposure indicated the fate of excitation energy in PS II (Schreiber and Klughammer, 2008), where Y(NPQ) in particular was associated with the quantum yield of regulated energy dissipation in PS II. The higher value of NPQ suggested a high photoprotective capacity, whereas a higher value of Y(NO) reflected the inability of the microalgal system to protect PS II damage under Se stress beyond 50 mg L^{-1}. Thus, high Y (NPQ) values can possibly compensate for the decrease in Y(II) and even a lowering of Y(NO). Our data are in tune with reports of Klughammer and Schreiber (Klughammer and Schreiber, 2008), that the PS II inhibition occurred under stress conditions, and the decrease in Y(II) was compensated by the corresponding increase of Y(NO).

The qP and qN are the coefficients of respective photochemical fluorescence quenching and non-photochemical fluorescence quenching. The qE denotes energy-dependent quenching linked with the PS II reaction centre excitation rate and light-induced proton transport into the thylakoid lumen. The significant decrease in qP (Fig. 2G) may be attributed to the reduction in the fraction of open PS II reaction centers that limited the proportion of captured light energy. The qL was associated with the PS II redox state, indicating the fraction of the open reaction centre (Baker, 2008). The assessment of dissipation energy pathways demonstrated that the *D. salina* exposed beyond 50 mg L^{-1} Se (100, 200, and 500 mg L^{-1}) was not used in photochemical and non-photochemical processes, as shown by the decrease in qP, qN, and qL on 6th d after Se exposure (Fig. 2G, H, and I).

3.3. Quantification of Chl a using flow cytometry (FCM)

A decline in the photosynthetic status of *D. salina* cells beyond 50 mg L^{-1} Se exposure prompted to monitor the effect of Se concentrations on chlorophyll content by FCM in NR-stained *D. salina* cells. The FCM signals based on APC A channel fluorescence in *D. salina* cells exposed to higher Se concentrations revealed altered Chl *a* fluorescence (Fig. 3). These results demonstrated that the decrease in photosynthetic activity at higher Se levels was manifested by a decline in chlorophyll levels to 92.96 %, 91.95 % and 91.14 % in 100, 200, and 500 mg L^{-1} Se respectively, as compared to the control (96.54 %), 25 mg L^{-1} (95.06) and 50 mg L^{-1} (94.84 %). Likewise, FCM analysis for *Tetraselmis* cells under nitrogen deprivation and high irradiance conditions caused declined chlorophyll levels (Dammak et al., 2021). These findings are in agreement with the previous study highlighting the detrimental impact of stress on photosynthetic machinery (Yao et al., 2016).

3.4. Effect of Se on Raman spectra in D. salina cells

Carotenoids serve as auxiliary light-harvesting pigments, non-photochemical quenching modifiers, and reactive oxygen species

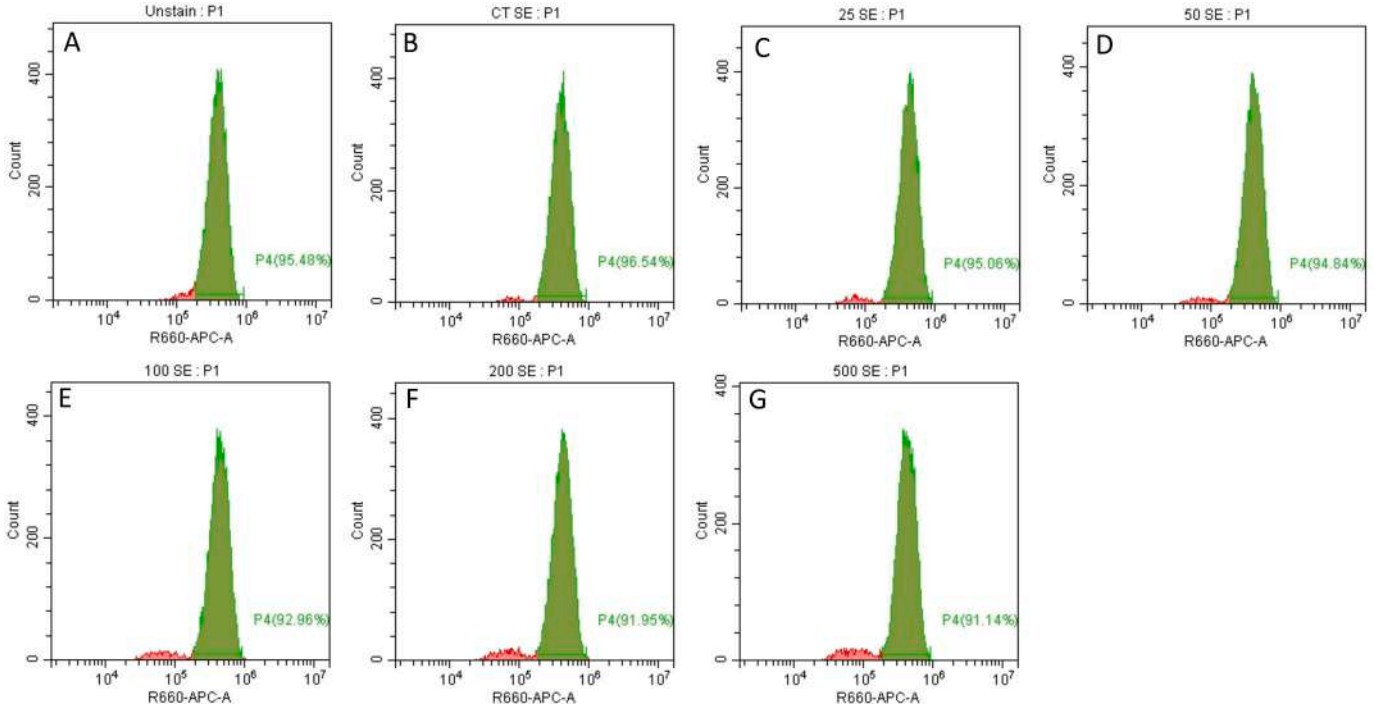

Fig. 3. Effect of varying levels of Se on chlorophyll content of *D. salina* using flow cytometry: (A) unstained cells, (B) control (− Se), (C) 25, (D) 50, (E) 100, (F) 200 and, (G) 500 mg L^{-1}.

scavengers in photosynthetic organisms. The Raman spectra of *D. salina* cells exposed to varying concentrations of Se (0–500 mg L^{-1}) were recorded, and the characteristic bands of carotenoids 1000–1020 cm^{-1}, 1150–1170 cm^{-1}, and 1500–1550 cm^{-1} on exposure to visible laser excitation are shown in Fig. 4. The inherently weak Raman signal was negated as background noise. There were other medium intensity peaks, of which 1003–1010 and 1189–1197 cm^{-1} having a slight deviation of 7–8 cm^{-1} from the Raman peaks, corresponding to related carotenoid, β-carotene, and astaxanthin. The strong Raman shifts at 1156 cm^{-1} (C—C stretching vibration) and 1513–1515 cm^{-1} (C═C stretching vibration) were observed in all Se exposed *D. salina* cells. The displacement of the similar peaks at increasing concentrations of Se was conclusive of the changes in the type of carotenoid, particularly the astaxanthin component of *D. salina*. The significant change in Raman

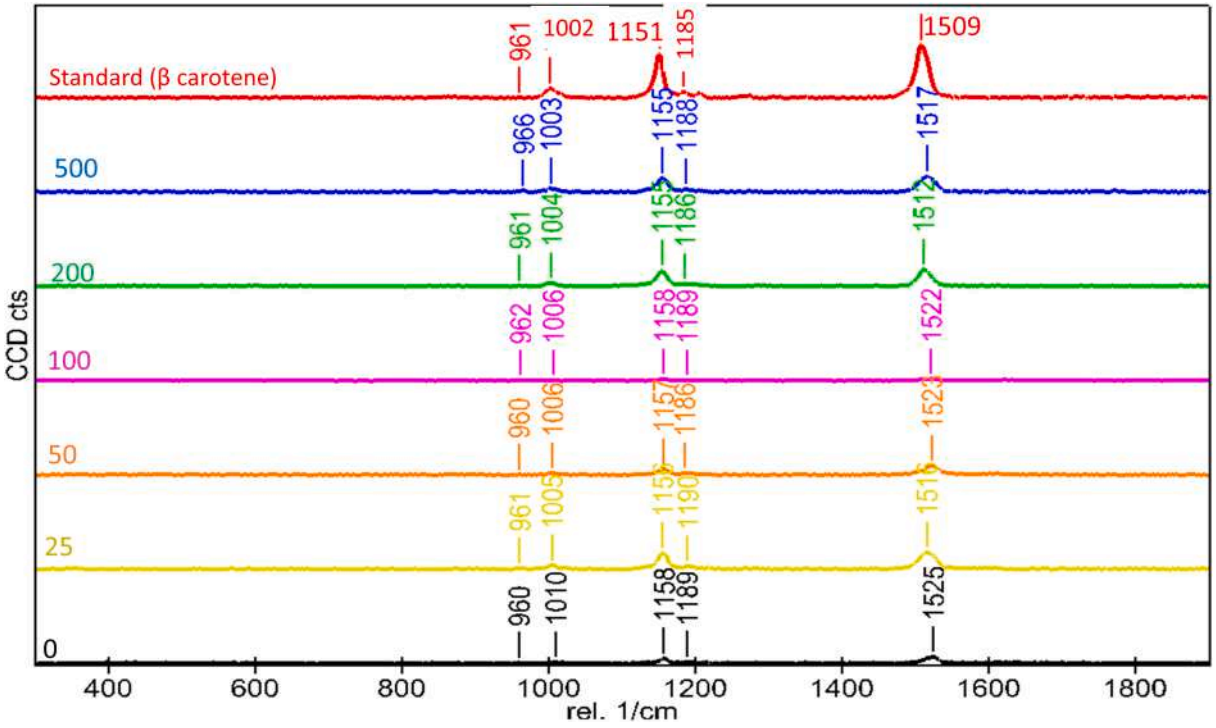

Fig. 4. Raman spectra of standard carotenoid, and *D. salina* exposed to varying levels Se (0–500 mg L^{-1}).

Shift and peak intensity of three corresponding Raman lines at 1003–1010, 1155–1158, 1194–1197, and 1513–1525 cm^{-1} indicated heterogeneity in the carotenoid production across varying concentrations of Se. The Raman spectrum for Se treated *D. salina* cells was very similar to the Raman spectra of the astaxanthin standard (Fig. 4), as reported by Shao et al. (Shao et al., 2019). In another study, the signature peak positions from the reference standards of lycopene (1004 cm^{-1} C-CH_3, 1155 cm^{-1} C—C and 1519 cm^{-1} C═C), xanthophyll (1005 cm^{-1} C-CH_3, 1157 cm^{-1} C—C, and 1525 cm^{-1} C═C), and β-carotene (1010 cm^{-1} C-CH_3, 1158 cm^{-1} C—C, and 1518 cm^{-1} C═C) recorded (Winters et al., 2013) were in congruence with our data. However, additional factors may also be showing interference with overlapping bands of other components such as lipids, proteins, etc. Therefore, it was concluded that the selective peaks at 1522–1526 cm^{-1} (C═C) were specific for the relative changes in carotenoids. It can be seen that in addition to the standard astaxanthin observed at 1520 cm^{-1} (C═C shift) there was an apparent deviation of 5–6 cm^{-1}.

3.5. Ultrastructure of D. salina cells under Se exposure and intracellular Se accumulation

The exponentially grown *D. salina* cells exposed to 200 mg L^{-1} Se were examined for the ultrastructural changes in microalgal cells at 4th d exposure in reference to the control, using TEM (Fig. 5). It was apparent that control cells possessed intact nucleus, eye spot, thylakoid, endoplasmic reticulum, mitochondria, and Golgi complex (Fig. 5A and C). However, the 200 mg L^{-1} Se exposed cells showed drastic change in ultrastructural details of major organelles including, the nucleus, thylakoid, mitochondria and vacuoles along with accumulation of Se in cytoplasm (Fig. 5B). Likewise, the higher level of Se exposed *D. salina* cells resulted in ultrastructural variations, showing organellar destruction (Renouva et al., 2007). The predominant changes in the ultrastructure of *D. tertiolecta* caused by the selenate and selenite toxicity were reported (Wong and Oliveira, 1991) and ascribed to damage in the energy transducing systems. Other microalga *C. sorokiniana* showed disoriented thylakoids with less dense stroma, having plastoglobules at higher Se levels (Gojkovic et al., 2014). The acclimation of *D. salina* to high salt concentration has probably resulted in increased Se tolerance, as 50 mg L^{-1} exposure did not become unfavorable for photoautotrophic growth. However, beyond 50 mg L^{-1} of Se exposure, the ultrastructural details of the *D. salina* cells evidenced its impact on the cellular organelles. Therefore, we have selected only control as well as 200 mg L^{-1} Se exposed *D. salina* cells because the prominent changes in the ultrastructure of the cells became apparent at this concentration.

Ultrastructural changes in *D. salina* led us to investigate intracellular Se accumulation, as it was supposed to reveal the toxicity threshold. The basal level of Se in *D. salina* cells was 35 μg g^{-1} DW in contrast to other microalgal species such as *Nannochloropsis oceanica* (10 μg g^{-1} DW) (Guimarães et al., 2021), and *Haematococcus pluvialis* (11 μg g^{-1} DW) (Zheng et al., 2017). The differences in the basal levels of the microalgae may be attributed to species specificity itself. In 25 and 50 mg L^{-1} Se exposed *D. salina* cells, the intracellular accumulation occurred up to 52 μg g^{-1} DW (1.4 fold) and 65 μg g^{-1} DW (1.8 fold), respectively in comparison to control (Fig. 5E). It is noteworthy that the Se accumulation in *D. salina* up to a certain level may be used as a food and feed supplement. An absolute recommended dose for dietary Se intake will be determined by geographical location, the dietary status of the population and maximization of selenoenzymes activity. The Recommended Dietary Allowance (RDA) for adult population are 55 μg day^{-1} (United States), 60–75 μg day^{-1} (United Kingdom and Belgium) and populations of the world, deficient in Se intake (Waegeneers et al., 2013). Therefore, it is suggested that the incorporation of selenoproteins through fortified Se enriched *D. salina* may be used in the future after toxicity evaluation of such biomass and compliance with the safety standards. The *D. salina* cells showed healthy status up to 50 mg L^{-1} Se as reflected by *Fv/Fm* and Chl *a* content. However, with the increase in Se up to 200 mg L^{-1}, the intracellular accumulation reached 2262 μg g^{-1} DW (64.2 fold) over the basal level causing apparent toxicity to cells as reflected by photo pigments and even ultrastructural details showing disrupted thylakoids and other organelles (Fig. 5B and D). Zheng et al. (Zheng et al., 2017)

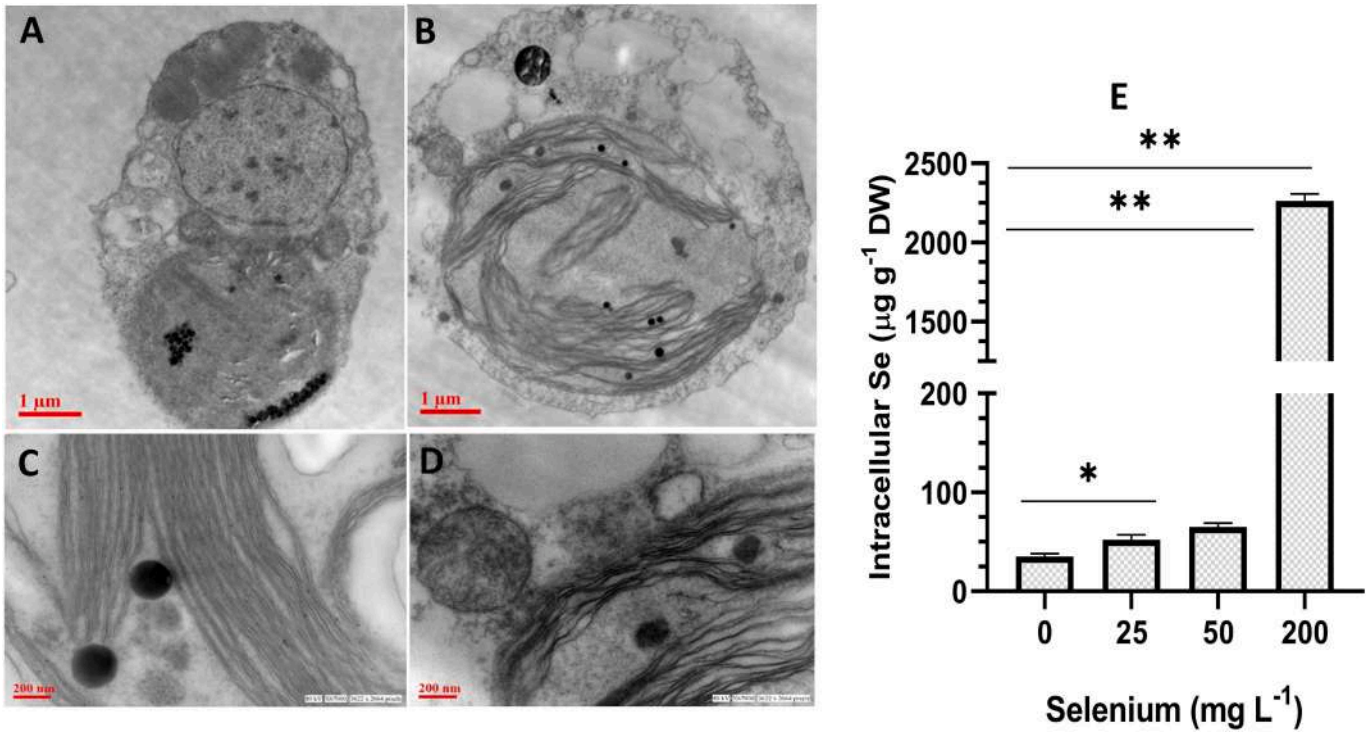

Fig. 5. Ultrastructural details of *D. salina* cell, observed under transmission electron microscopy (TEM): (A) control cell (intact organelles), (B) cell exposed to 200 mg L^{-1} Se showing disruptive cell organelles with accumulated Se (C) control cell with intact thylakoid and (D) 200 mg L^{-1} treated cell with deteriorated thylakoid, and (E) intracellular Se accumulation in *D. salina*.

reported that *H. pluvialis* accumulated the highest organic Se at 13 mg L^{-1} of selenite, and so establishing it to be an effective concentration for biomass production. In *C. pyrenoidosa*, the highest total Se content was found to be 435 μg g^{-1} DW, along with the maximum accumulation of organic Se at 337 μg g^{-1} DW, indicating its efficacy as an efficient Se accumulator (Schrauzer, 2003). Likewise, the study with *C. vulgaris* revealed the highest total Se content at 857 μg g^{-1} DW with maximum accumulation for organic selenium recording at 316 μg^{-1} g DW at 75 mg L^{-1} Se concentration (Sun et al., 2014).

3.6. Effect of Se on intracellular ROS generation

Abiotic stress induces a powerful intrinsic antioxidant mechanism in photosynthetic cells that controls ROS generation. The 2′-7′ dichlorodihydrofluorescein diacetate (DCFH-DA) is a frequently used stain to measure ROS accumulation in living cells. Cells emitted red (autofluorescence) having lesser ROS accumulation and green due to the oxidation of DCFH-DA with higher ROS species generating fluorescent DCF (dichlorofluorescein) molecule. The red colored *D. salina* cells exposed to 0, 25, and 50 mg L^{-1} Se (Fig. 6) indicated minimal ROS accumulation, whereas the green colored *D. salina* cells exposed to 100, 200, and 500 mg L^{-1} Se showed higher ROS accumulation (Fig. 6). The growth retardation in *D. salina* cells exposed to Se above 50 mg L^{-1} may be ascribed to increases in ROS and lipid peroxidation, which are well-known oxidative stress markers. In an earlier report, a lower concentration of Se (75 mg L^{-1}) stimulated the growth of microalga *C. vulgaris* (Sun et al., 2014) by decreasing ROS generation and lipid peroxidation in the cells, whereas exposure to a higher concentration of Se (100 mg L^{-1}) led to oxidative stress by increasing the ROS content and lipid peroxidation (Sun et al., 2014).

3.7. Effect of selenium on antioxidative enzymes (SOD and CAT)

Excess ROS accumulation and oxidative stress resulting from elevated Se concentration were countered with antioxidative enzymes as part of the defense mechanism. The SOD and CAT activity in *D. salina* cells exposed to varying Se concentrations were investigated in native PAGE. The CAT activity staining showed seven differentially expressed isoforms. However, all these isoforms were expressed in 50, and 100 mg L^{-1} Se treated *D. salina* cells (Fig. 7A). Among seven isoforms, CAT6 expressed prominently in all treatments, as well as in the control, and its expression increased significantly with a rise in Se levels. The other isoforms showed weak expression patterns and varied with treatment levels. The CAT1 and CAT2 expressions were similar in control (0), 25, 50, and 100 mg L^{-1} Se treated cells, whereas negligible expressions were recorded in 200 and 500 mg L^{-1} treated cells. The expression of CAT3 was only observed at 50, 100, and 200 mg L^{-1} Se treated *D. salina* cells. The CAT4 expression increased with increasing Se concentrations. CAT5 expressed constitutively in each treated and control cell, whereas CAT7 expressed better in 50 and 100 mg L^{-1} Se exposed *D. salina* cells. However, its expression was negligible in control, 25, 200, and 500 mg L^{-1} Se treated cells. The differential expression of CAT isoforms may be attributed to varying levels of ROS in response to Se treatments. Three isoforms were reported in *C. reinhardtii* irrespective of culture conditions (Kato et al., 1997). On the contrary, a decrease in CAT activity in *C. pyrenoidosa* at higher Se concentrations has been reported (Sun et al., 2014).

The SOD activity also revealed considerable variation in the banding profile of five isoforms with regard to Se treatments (Fig. 7B). The expression of SOD1 increased significantly from control to 100 mg L^{-1} Se exposed *D. salina* cells and declined at 200 and 500 mg L^{-1} Se levels. Interestingly, the SOD2, SOD3, and SOD4 expressed constitutively across all the treatment levels. An increase in the expression of SOD5 was recorded with increasing Se concentrations. Such differential expression of SOD isoforms under varying Se concentrations clearly indicated Se dose-specific isoforms expression. Interestingly, *D. salina* CCAP 19/18, subjected to N, Mn, Zn, and Fe stress, showed eight isoforms of SODs (Saha et al., 2013). The differential expression of

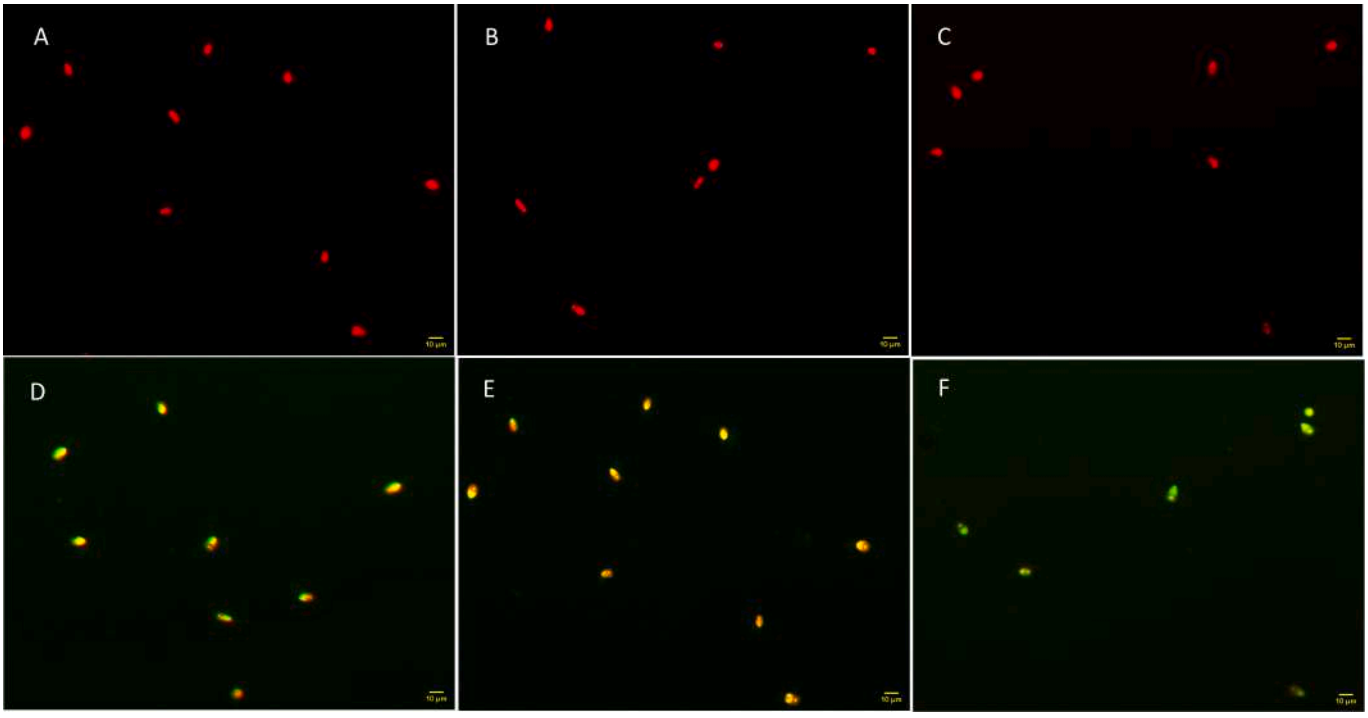

Fig. 6. Fluorescent microscopic analysis of *D. salina*, exposed to varying Se levels: 0 (A), 25 (B), 50 (C), 100 (D), 200 (E) and, 500 mg L^{-1} showing ROS accumulation. *D. salina* cells stained with DCFH-DA, emitted red (autofluorescence) having lesser ROS accumulation, and green due to the oxidation of DCFDA with higher ROS species, generating fluorescent DCF molecule (green). (For interpretation of the references to color in this figure legend, the reader is referred to the web version of this article.)

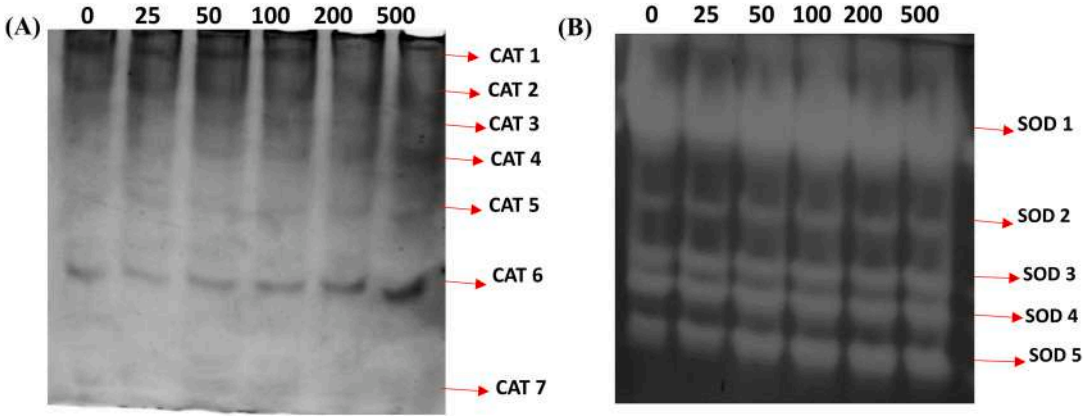

Fig. 7. In-gel assay of catalase (A) and SOD enzyme activity (B) of *D. salina* cells exposed to varying Se levels (0, 25, 50, 100, 200, 500 mg L^{-1}).

antioxidative enzymes such as CAT and SOD were previously studied in *D. salina* cells under varying salinity levels (Singh et al., 2019). These workers also reported eight isoforms of SODs under salinity stress, wherein few isoforms expressed constitutively and some differentially.

3.8. Effect of Se on lipid accumulation in D. salina cells

The neutral lipids in NR-stained *D. salina* cells exposed to Se (0–500 mg L^{-1}) concentration were visualized using confocal microscopy (Fig. 8A). The increase in Se concentration from 25 mg L^{-1} to 500 mg L^{-1} led to rise in neutral lipid accumulation. Increase in the number of cytoplasmic lipid droplets was recorded at higher Se levels (100, 200, and 500 mg L^{-1}), accompanied by change in the shape of *D. salina* cells from elongated to semi-spherical. The fluorescence intensity (AU) vs. Se concentration was also plotted (Fig. 8B). It showed a rise in lipid accumulation with increases in Se concentrations. However, increase in lipid accumulation was not significant up to 50 mg L^{-1} Se exposure, whereas a significant rise in lipid accumulation was recorded at higher Se concentrations. These observations pointed out that 50 mg L^{-1} Se exposure was not acting as an effective lipid inductor in the *D. salina* strain. In contrast to our observations, the lower doses of the Se (10–20 mg L^{-1}) enhanced the lipid production in *D. tertiolecta* more than two fold (Perečinec et al., 2022). This difference between the two strains of *Dunaliella* sp. may be ascribed to strain specificity towards the Se, rendering *D. salina's* inherent capacity to withstand stress. We have already reported higher lipid accumulation in this strain beyond 2 M NaCl exposure, showing its ability to tolerate salinity stress (Singh et al., 2019).

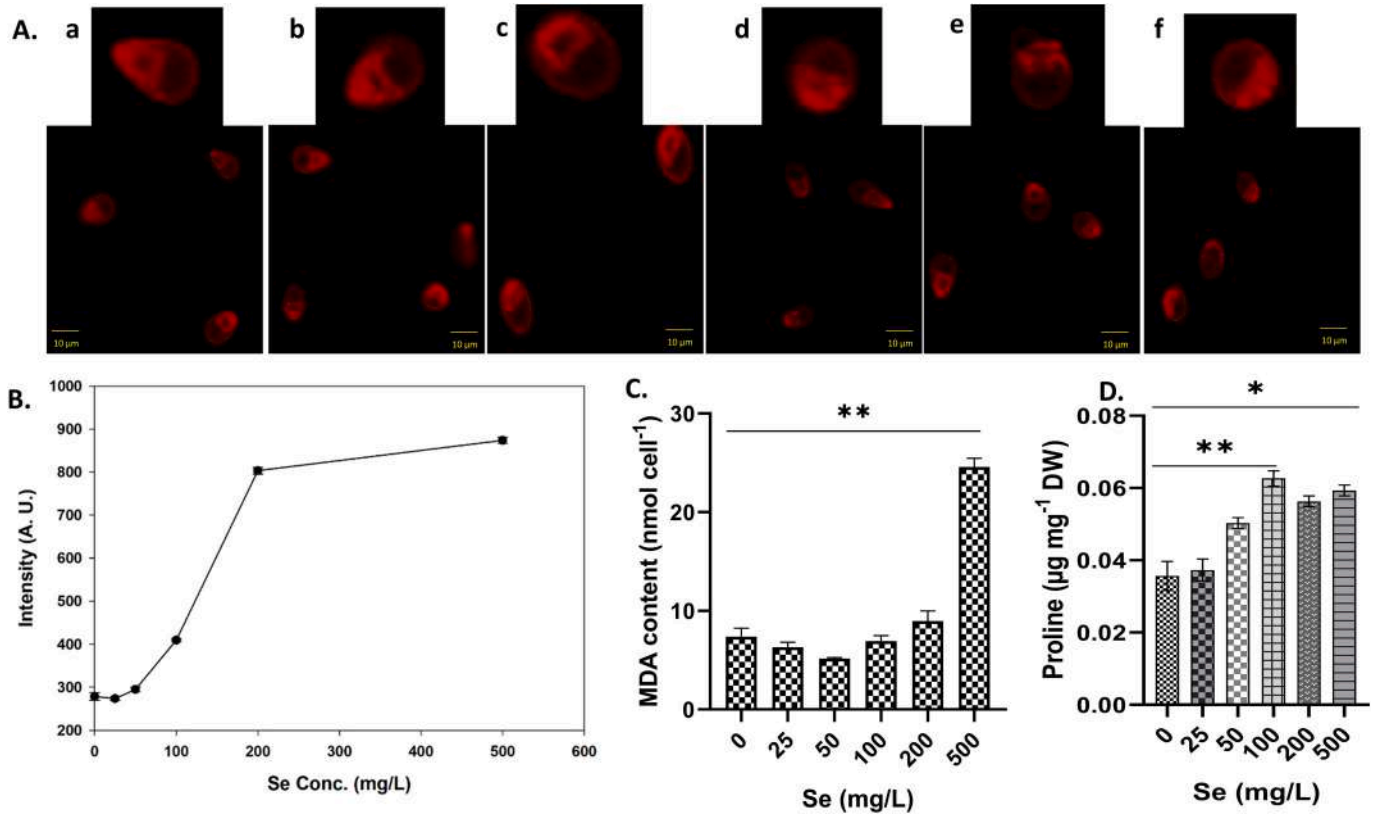

Fig. 8. (A) Fluorescence micrograph of Nile Red stained *D. salina cells exposed* to selected Se levels (a), 25 (b), 50 (c), 100 (d), 200 (e) and 500 (f); (B) depicts Nile Red fluorescence of *D. salina* cells (C) MDA and (D) Proline content in *D. salina* cells exposed to Se (0–500 mg L^{-1}). (For interpretation of the references to color in this figure legend, the reader is referred to the web version of this article.)

3.9. Effect of Se on lipid peroxidation (LPO) and proline content

The impact of varying levels of Se on lipid peroxidation of *D. salina* is represented in Fig. 8C. There was a marginal decline in LPO level (5.15 nmol cell^{-1}) of 50 mg L^{-1} Se exposed cells in comparison to the control (7.39 nmol cell^{-1}) indicating no Se stress at lower levels. The rise in LPO from 6.93 to 8.69 nmol cell^{-1} at 100 and 200 mg L^{-1} Se treated cells may be attributed to stress caused by higher Se doses. The cells exposed to 500 mg L^{-1} Se showed 2.8 fold rise in LPO over that of 200 mg L^{-1} Se exposed cells. Cells exposed to 500 mg L^{-1} Se had 4.77 fold rise in lipid peroxidation with respect to cells exposed to 50 mg L^{-1} Se. Overall data on Se exposure to *D. salina* cells suggested that Se at lower concentration help ROS scavenging by decreasing LPO, whereas at higher Se level, the induced LPO leads to membrane damage through oxidative stress and ROS generation.

Higher selenium tolerance might be attributed to an increase in the proline content of *D. salina* cells. The key role of proline was to maintain the metabolic status of the stressed cells. Therefore, in this study, the accumulation of proline at varying concentrations of Se was monitored (Fig. 8D). The target strain exposed to 25 mg L^{-1} could not induce a significant level of proline content. However, 50 mg L^{-1} exposed *D. salina* cells registered a 1.41 fold rise in proline content over the control and 1.75 fold at 100 mg L^{-1} Se exposed cells. An increase in Se concentrations beyond 100 mg L^{-1} did not cause a further rise in intracellular proline content. The proline is known for its multifunctional role as osmoticum, a store of energy in the form of ATP (Atkinson, 1977). Therefore, a rise in proline content at 50 mg L^{-1} Se played a role in scavenging the stress.

3.10. Conclusions

This study demonstrates impact of Se on photoautotrophic growth of *D. salina* and its bioaccumulation. *D. salina* experienced stress beyond 50 mg L^{-1} Se exposure, evident from the decline in photosynthetic activity and increased ROS, LPO, intracellular proline, and neutral lipid contents. The differential expression of various SOD and CAT isoforms played a pivotal role. As Se is a requirement in biomedicine, Se-enriched *D. salina* biomass may be used as food and feed supplement after evaluating the toxicity assay. Also, the inherent capacity of *D. salina* to tolerate higher Se levels may be used for the bioremediation of Se.

Supplementary data to this article can be found online at https://doi.org/10.1016/j.marpolbul.2023.114842.

CRediT authorship contribution statement

Singh, P and Singh, S: Design of the experiments, execution, methodology characterization and experimentation data collection, analysis and ms writing; Maurya, P., Mohanta, A., Khadin S. R., and, Singh, S. R.: methodology characterization and experimentation data collection, Dubey, H.: Data analysis/interpretation, Pandey, A.: Raman spectroscopy, Singh, A. K.: Draft preparation and manuscript editing, Asthana, R. K.: Sample collection from hypersaline Sambhar lake, Rajasthan, India, conceptualization and the direction in designing, writing of ms and compilation. All authors approved the final manuscript.

Declaration of competing interest

There is no conflict of interest among authors.

Data availability

Data will be made available on request.

Acknowledgements

We gratefully acknowledge the Head and Coordinators of CAS in Botany, DST-FIST, ISLS, CDC BHU for providing research facilities. The financial supports are also acknowledged by PS (DSKPDF; No. F.4-2/2006(BSR)/BL/19-20/162), SS (DBT/BHU-ISLS/2020-21/Ph.D/Sept. 2020/02), PM (19/06/2016(i) EU-V), AM (09/013(0733)/2017—EMR-I), HD (DBTHRDPMU/JRF/BET—20/I/2020/AL/366), and IoE (SCHEME No. 6031).

References

Atkinson, D.E., 1977. Cellular Energy Metabolism and Its Regulation. Academic Press, New York.
Becker, E.W., 2007. Micro-algae as a source of protein. Biotechnol. Adv. 25 (2), 207–210.
Baker, N.R., 2008. Chlorophyll fluorescence: a probe of photosynthesis in vivo. Annu. Rev. Plant Biol. 59, 89.
Bates, L.S., Waldren, R.P., Teare, I.D., 1973. Rapid determination of free proline for water-stress studies. Plant Soil 39 (1), 205–207.
Bradford, M.M., 1976. A rapid and sensitive method for the quantitation of microgram quantities of protein utilizing the principle of protein-dye binding. Anal. Biochem. 72 (1–2), 248–254.
Butler, W.L., 1978. Energy distribution in the photochemical apparatus of photosynthesis. Annl. Rev. Plant Physiol. 29 (1), 345–378.
Dammak, M., Hlima, H.B., Elleuch, F., Pichon, C., Michaud, P., Fendri, I., Abdelkafi, S., 2021. Flow cytometry assay to evaluate lipid production by the marine microalga Tetraselmis sp. using a two stage process. Renew. Energy 177, 280–289.
De Morais, E.G., Murillo, A.M., Lens, P.N., Ferrer, I., Uggetti, E., 2022. Selenium recovery from wastewater by the green microalgae Chlorella vulgaris and Scenedesmus sp. Sci. Total Environ. 851, 158337.
Dhindsa, R.S., Matowe, W., 1981. Drought tolerance in two mosses: correlated with enzymatic defence against lipid peroxidation. J. Exp. Bot. 32, 79–91.
Ekelund, N.G., Danilov, R.A., 2001. The influence of selenium on photosynthesis and" light-enhanced dark respiration"(LEDR) in the flagellate Euglena gracilis after exposure to ultraviolet radiation. Aquat. Sci. 63, 457–465.
El-Baz, F.K., Salama, A.A., Hussein, R.A., 2020. Dunaliella Salina microalgae oppose thioacetamide-induced hepatic fibrosis in rats. Toxicol. Rep. 7, 36–45.
Geoffroy, L., Gilbin, R., Simon, O., Floriani, M., Adam, C., Pradines, C., Cournac, L., Garnier-Laplace, J., 2007. Effect of selenate on growth and photosynthesis of Chlamydomonas reinhardtii. Aquat. Toxic. 83 (2), 149–158.
Gojkovic, Ž., Garbayo, I., Ariza, J.L.G., Márová, I., Vílchez, C., 2015. Selenium bioaccumulation and toxicity in cultures of green microalgae. Algal Res. 7, 106–116.
Gojkovic, Ž., Vílchez, C., Torronteras, R., Vigara, J., Gómez-Jacinto, V., Janzer, N., Marova, I., Garbayo, I., Luis-Gomez, Ariza.J., 2014. Effect of selenate on viability and selenomethionine accumulation of Chlorella sorokiniana grown in batch culture. Sci. World Journal. 1–14.
Gómez-Jacinto, V., Navarro-Roldán, F., Garbayo-Nores, I., Vílchez-Lobato, C., Borrego, A.A., García-Barrera, T., 2020. In vitro selenium bioaccessibility combined with in vivo bioavailability and bioactivity in se-enriched microalga (Chlorella sorokiniana) to be used as functional food. J. Funct. Foods 66, 103817.
Gobi, N., Vaseeharan, B., Rekha, R., Vijayakumar, S., Faggio, C., 2018. Bioaccumulation, cytotoxicity and oxidative stress of the acute exposure selenium in Oreochromis mossambicus. Ecotoxicol. Environ. Saf. 30 (162), 147–159.
Gopi, N., Rekha, R., Vijayakumar, S., Liu, G., Monserrat, J.M., Faggio, C., Nor, S.A., Vaseeharan, B., 2021. Interactive effects of freshwater acidification and selenium pollution on biochemical changes and neurotoxicity in Oreochromis mossambicus. Comp. Biochem. Physiol. Part C: Toxicol. Pharmacol. 1 (250), 109161.
Guimarães, B.O., de Boer, K., Gremmen, P., Drinkwaard, A., Wieggers, R., Wijffels, R.H., D'Adamo, S., 2021. Selenium enrichment in the marine microalga nannochloropsis oceanica. Algal Res. 59, 102427.
Helliwel, B., Gutteridge, J.M.C., 1999. Free Radical in Biology and Medicine. Oxford University Press, New York.
Handy, D.E., Joseph, J., Loscalzo, J., 2021. Selenium, a micronutrient that modulates cardiovascular health via redox enzymology. Nutrients 13 (9), 3238.
He, Y.Y., Häder, D.P., 2002. UV-B-induced formation of reactive oxygen species and oxidative damage of the cyanobacterium anabaena sp.: protective effects of ascorbic acid and N-acetyl-L-cysteine. J. Photochem. Photobiol. B Biol. 66 (2), 115–124.
Jiang, L., Lu, Y., Zheng, L., Li, G., Chen, L., Zhang, M., Zhang, Y., 2020. The algal selenoproteomes. BMC Genom. 21 (1), 1–16.
Jiang, X., Yang, L., Wang, Y., Jiang, F., Lai, J., Pan, K., 2023 Feb 13. Proteomics provide insight into the interaction between selenite and the microalgae Dunaliella Salina. Processes. 11 (2), 563.
Kato, J., Yamahara, T., Tanaka, K., Takio, S., Satoh, T., 1997. Characterization of catalase from green algae Chlamydomonas reinhardtii. J. Plant Physiol. 151, 262–268.
Klughammer, C., Schreiber, U., 2008. Complementary PS II quantum yields calculated from simple fluorescence parameters measured by PAM fluorometry and the saturation pulse method. PAM Appl. Notes 1 (2), 201–247.
Letavayová, L., Vlčková, V., Brozmanová, J., 2006. Selenium: from cancer prevention to DNA damage. Toxicology 227 (1–2), 1–14.
Loscalzo, J., 2014. Keshan disease, selenium deficiency, and the selenoproteome. N. Engl. J. Med. 370 (18), 1756–1760.
Myers, J., Kratz, W., 1955. Relations between pigment content and photosynthetic characteristics in a blue-green alga. J. Gen. Physiol. 39, 11–22.
Perečinec, M.G., Babić, S., Čižmek, L., Selmani, A., Popović, N.T., Sikirić, M.D., Strunjak-Perović, I., Čož-Rakovac, R., 2022. Selenite as a lipid inductor in marine microalga

Dunaliella tertiolecta: comparison of one-stage and two-stage cultivation strategies. Appl. Biochem. Biotech. 194 (2), 930–949.
Pilon-Smits, E.A., 2019. On the ecology of selenium accumulation in plants. Plants 8 (7), 197.
Renouva, Y.A., Aizdaicher, N.A., Khristoforova, N.K., Reunov, A.A., 2007. Effects of selenium on growth and ultrastructure of the marine unicellular alga Dunaliella Salina (Chlorophyta). Russ. J. Mar. Biol. 33 (2), 125–132.
Saha, S.K., Moane, S., Murray, P., 2013. Effect of macro-and micro-nutrient limitation on superoxide dismutase activities and carotenoid levels in microalga Dunaliella salina CCAP 19/18. Bioresour. Technol. 147, 23–28.
Saito, Y., 2021. Selenium transport mechanism via selenoprotein P—its physiological role and related diseases. Front. Nutr. 8, 685517.
Schrauzer, G.N., 2003. The nutritional significance, metabolism and toxicology of selenomethionine. Adv. Food Nutr. Res. 47 (1), 73–112.
Schreiber, U., Klughammer, C., 2008. Non-photochemical fluorescence quenching and quantum yields in PS I and PS II: analysis of heat-induced limitations using Maxi-Imaging-PAM and Dual-PAM-100. In: PAM Application Notes, 1, pp. 15–18.
Shao, Y., Gu, W., Jiang, L., Zhu, Y., Gong, A., 2019. Study on the visualization of pigment in haematococcus pluvialis by Raman spectroscopy technique. Sci. Rep. 9 (1), 1–9.
Singh, P., Khadim, R., Singh, A.K., Singh, U., Maurya, P., Tiwari, A., Asthana, R.K., 2019. Biochemical and physiological characterization of a halotolerant Dunaliella Salina isolated from hypersaline Sambhar LakeIndia. J. Phycol. 55 (1), 60–73.
Sohrin, Y., Bruland, K.W., 2011. Global status of trace elements in the ocean. TrAC, trendsAnal. Chem. 30 (8), 1291–1307.
Sui, Y., Vlaeminck, S.E., 2020. Dunaliella microalgae for nutritional protein: an undervalued asset. Trends Biotechnol. 38 (1), 10–12.
Sun, X., Zhong, Y., Huang, Z., Yang, Y., 2014. Selenium accumulation in unicellular green alga Chlorella vulgaris and its effects on antioxidant enzymes and content of photosynthetic pigments. Plos One. 9 (11), e112270.
Thomson, C.D., 2004. Assessment of requirements for selenium and adequacy of selenium status: a review. Eur. J. Clin. Nutr. 58 (3), 391–402.
Turanov, A.A., Xu, X.M., Carlson, B.A., Yoo, M.H., Gladyshev, V.N., Hatfield, D.L., 2011. Biosynthesis of selenocysteine, the 21st amino acid in the genetic code, and a novel pathway for cysteine biosynthesis. Adv. Nutr. 2 (2), 122–128.
Waegeneers, N., Thiry, C., De Temmerman, L., Ruttens, A., 2013. Predicted dietary intake of selenium by the general adult population in Belgium. Food Addit Contam: Part A 30 (2), 278–285.
Wang, J., Zhao, S., Yang, L., Gong, H., Li, H., Nima, C., 2021. Assessing the health loss from Kashin-Beck disease and its relationship with environmental selenium in Qamdo district of Tibet, China. Int. J. Environ. Res. 18 (1), 11.
White, P.J., Bowen, H.C., Parmaguru, P., Fritz, M., Spracklen, W.P., Spiby, R.E., Broadley, M.R., 2004. Interactions between selenium and sulphur nutrition in Arabidopsis thaliana. J. Exp. Bot. 55 (404), 1927–1937.
Weydert, C.J., Cullen, J.J., 2010. Measurement of superoxide dismutase, catalase and glutathione peroxidase in cultured cells and tissue. Nat. Protoc. 5 (1), 51–66.
WHO, 2005. In: Selenium, Chapter 10 World Health Organization, Geneva, pp. 191–216.
Winters, Y.D., Lowenstein, T.K., Timofeeff, M.N., 2013. Identification of carotenoids in ancient salt from Death Valley, Saline Valley, and searles Lake, California, using laser raman spectroscopy. Astrobiology 13 (11), 1065–1080.
Wong, D., Oliveira, L., 1991. Effects of selenite and selenate toxicity on the ultrastructure and physiology of three species of marine microalgae. Can. J. Fish. Aquat. 48 (7), 1201–1211.
Yao, S., Lu, J., Sárossy, Z., Baggesen, C., Brandt, A., An, Y., 2016. Neutral lipid production in Dunaliella Salina during osmotic stress and adaptation. J. Appl. Phycol. 28 (4), 2167–2175.
Yilancioglu, K., Cokol, M., Pastirmaci, I., Erman, B., Cetiner, S., 2014. Oxidative stress is a mediator for increased lipid accumulation in a newly isolated Dunaliella Salina strain. PloS One. 9 (3), e91957.
Zhang, B., Duan, G., Fang, Y., Deng, X., Yin, Y., Huang, K., 2021. Selenium (IV) alleviates chromium (VI)-induced toxicity in the green alga Chlamydomonas reinhardtii. Environ. Poll. 272, 116407.
Zhang, J., Saad, R., Taylor, E.W., Rayman, M.P., 2020. Selenium and selenoproteins in viral infection with potential relevance to COVID-19. Redox Biol. 37, 101715.
Zhang, X., Liu, R.P., Cheng, W.H., Zhu, J.H., 2019. Prioritized brain selenium retention and selenoprotein expression: nutritional insights into Parkinson's disease. Mech. Ageing Dev. 180, 89–96.
Zheng, Y., Li, Z., Tao, M., Li, J., Hu, Z., 2017. Effects of selenite on green microalga Haematococcus pluvialis: bioaccumulation of selenium and enhancement of astaxanthin production. Aquat. Toxicol. 183, 21–27.
Zhong, Y., Cheng, J.J., 2017. Effects of selenite on unicellular green microalga Chlorella pyrenoidosa: bioaccumulation of selenium, enhancement of photosynthetic pigments, and amino acid production. J. Agric. Food Chem. 65 (50), 10875–10883.